20th Australasian Fluid Mechanics Conference
Perth, Australia
5-8 December 2016

Transient Analysis of Global Dominant Modes in Quasi-Static Magnetohydrodynamic Flows

O. G. W. Cassells, T. Vo and G. J. Sheard

Department of Mechanical and Aerospace Engineering
Monash University, Victoria 3800, Australia

Abstract

The global maximum transient amplifications of an electrically conducting fluid under the influence of a transverse magnetic field in square duct were investigated. A range of Hartmann numbers for $10 \leq Ha \leq 1000$ were tested at a fixed $Re = 5000$ to elucidate the processes through which transition from three-dimensional perturbation states at low magnetic field strengths give way to predominantly anisotropic two-dimensional structures at higher field strengths. Such flows are applicable to metallurgical processes where magnetic fields are used to dampen disturbances to increase homogeneity in material production, as well as in the cooling blankets of nuclear fusion reactors where instabilities can aid in improving convective heat transfer. Two regimes are identified for the scaling of maximum transient energy amplification; when perturbation structures are dominated by three dimensional variation in the vertical side-wall boundary layers a scaling of $G_{\max} \propto Ha^{-1.6}$ for $10 \leq Ha \leq 100$ was found, while scaling of $G_{\max} \propto Ha^{-0.37}$ over $150 \leq Ha \leq 1000$ occurs for when quasi-two-dimensional (Q2D) disturbances are prevalent. Through comparison with existing literature, the Q2D model of Sommeria & Moreau (1982) is shown to be valid for $Ha > 150$.

Introduction

Understanding the stability mechanisms of electrically conducting fluids under the influence of strong magnetic fields, known as magnetohydrodynamic (MHD) flows, has potentially significant implications to metallurgical processes, and more pertinently the viability of clean energy sources, such as magnetic confinement fusion reactors. For the latter, the strong transverse magnetic fields that exist to contain the plasma have a strong damping effect on the flow differentials in the adjacent liquid metal cooling blankets. As a result, efficient convective heat transport is adversely affected; a detriment to the thermal performance in maintaining safe operating temperatures of the reactor, and in the heat exchange process used in the production of electrical energy. To overcome these issues several works have been conducted with the aim of mechanically enhancing the convective heat transfer performance [3, 4]. However, these methods are not always practicable, and a further understanding of the underlying instability mechanisms which can aid in convection across a broader range of operational parameters are needed.

An issue with respect to the stability analysis of MHD flows in the limit of strong magnetic fields is the discrepancy between the critical regime parameters predicted through the growth of exponentially growing perturbations and that observed in experiments [5]. One explanation for this inconsistency is that non-orthogonality in transient amplifications can create a route for subcritical instability. In other words, the linearisation around a base state may predict asymptotically decaying eigenvalues, yet, interactions between suboptimal modes could result in sufficient non-linear transient amplifications to render the base flow unstable [6]. From a practical standpoint, the presence and structure of these optimal modes have been shown to form a fundamental part of fully developed turbulent flows [2]. Hence, by utilising the knowledge of the modal spatial characteristics, effective flow control strategies may be implemented such as, periodic suppression and/or excitation of electro-magnetic fields.

Due to their simplicity, existing literature has largely focused on the stability of Hartmann MHD flows (flow between parallel plates orthogonal to an applied magnetic field); that is, without consideration of the sidewall boundary layers, known as Shercliff layers, which form on duct sidewalls tangential to the magnetic field vector. One approach taken to examine the effects of the Shercliff layers on the stability of confined MHD flows was conducted by Pothérat [7]. A quasi-two-dimensional (Q2D) model developed by Sommeria & Moreau (1982) (hereafter SM82) [9] was utilised by assuming the flow outside of the Hartmann boundary layers, which form on the walls perpendicular to the magnetic field vector, are predominantly two-dimensional. It has been shown previously that this model remains sufficiently valid for magnetic interaction parameters $N \equiv Ha^2/Re \gg 1$, where Ha is the Hartmann number representing the effect of the Lorentz force on the flow, and Re is the Reynolds number [8]. From this work, global optimum transient growths were shown to become independent to three-dimensional (3D) wavenumbers and reach an asymptotic regime for $Ha \geq 200$. Subsequently, Krasnov *et al.* [5] employed 3D transient growth analysis to show an asymptotic scaling of global dominant modes following a $Ha^{-3/2}$ relation in the region of $10 \leq Ha \leq 50$ for $Re = 5000$ in square ducts.

To this date, it is not properly understood if Q2D models are accurate predictors of instability modes towards high magnetic field strengths, nor is there an extensive body of work on the physical structures which develop through their transition to a Q2D dominated state. It is therefore the focus of the present work to understand how and when specific linear transient amplifications present over a wide range of Ha, and the processes through which the 3D states at low magnetic field strengths give way to anisotropic 2D structures at higher field strengths in confined MHD flows.

Formulation

Problem Definition and Governing Equations

An electrically conducting fluid of conductivity σ, kinematic viscosity ν and density ρ flows through a duct having square cross-section with perfectly electrically insulated walls of width $2a$. The vertical and horizontal duct walls are located at $x = \pm a$ and $y = \pm a$, respectively. The flow is subject to a constant external homogeneous magnetic field $\boldsymbol{B_0} = B_0\boldsymbol{e}$ tangential to the vertical sidewalls such that $\boldsymbol{e} \equiv \langle 0,1,0 \rangle$ (see figure 1). The flow is driven by an imposed constant pressure gradient ∇p with no-slip conditions applied on all solid boundaries.

For sufficiently large B_0, the internal magnetic field induced by the motion of the conducting fluid, measured by the magnetic Reynolds number Re_m, can be rendered negligible in comparison to the externally applied field. This is a valid assumption for typical environments seen in industrial and

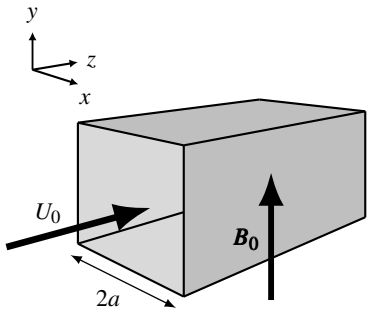

Figure 1: Schematic of flow configuration and parameters used in this study.

laboratory MHD applications [5]. It follows that, when taking proper scales for length a, pressure ρU_0^2, where U_0 is the peak inlet velocity, time a/U_0, magnetic field B_0 and lastly, for the electric potential aU_0B_0, the dimensionless quasi-static low-Re_m momentum and continuity equations can be expressed as

$$\frac{\partial \boldsymbol{V}}{\partial t} + (\boldsymbol{V}\cdot\boldsymbol{\nabla})\boldsymbol{V} = -\boldsymbol{\nabla}p + \frac{1}{Re}\nabla^2\boldsymbol{V} + \frac{Ha^2}{Re}(\boldsymbol{j}\times\boldsymbol{B_0}), \quad (1)$$

$$\boldsymbol{\nabla}\cdot\boldsymbol{V} = 0, \quad (2)$$

where $\boldsymbol{V}(x,y,z,t) = \langle u,v,w\rangle$ and $\boldsymbol{j} = -\boldsymbol{\nabla}\phi + \boldsymbol{V}\times\boldsymbol{B_0}$ are the velocity and electric current density vectors, respectively. Here ϕ is the electric scalar potential. Two independent dimensionless groupings exist in these governing equations. Namely, the Reynolds number $Re \equiv U_0 a/\nu$ representing the ratio of inertial to viscous forces in the flow, and the Hartmann number $Ha \equiv aB_0\sqrt{\sigma/\rho\nu}$ representing the effect of the Lorentz force on the flow in relation to geometric and fluid properties. In the present work, Hartmann numbers between $10 \leq Ha \leq 1000$ are investigated which significantly extends the range covered by [5]. The aim being to bridge the gap between 3D and Q2D models for transient growth analysis of optimal linear amplifications. Here a fixed Reynolds number of $Re = 5000$ is used both for comparison reasons with existing literature, but also as it is below the exponential instability limit found for hydrodynamic Poiseuille flows.

Transient growth analysis

A transient growth analysis is conducted by tracking the energy amplification over a finite time interval τ due to the evolution of linear three-dimensional infinitesimal perturbations $[\boldsymbol{V}_p,\phi_p,p_p](x,y,z,t) = (u',v',w',\phi',p')$ to a streamwise independent two-dimensional steady-state base flow $[\boldsymbol{V}_0,\phi_0,p_0] = (u(x,y),v(x,y),w(x,y),\phi(x,y),p(z))$. When the initial base state is subject to these perturbations, the solution takes the general form $[\boldsymbol{V},\phi,p] = (\boldsymbol{V}_0,\phi_0,p_0) + (\boldsymbol{V}_p,\phi_p,p_p)$. The perturbations are considered through the form of decoupled normal Fourier modes such that

$$[\boldsymbol{V}_p,\phi_p,p_p] = \left(\hat{u},\hat{v},\hat{w},\hat{\phi},\hat{P}\right)(x,y,t)\cdot e^{i\alpha z}, \quad (3)$$

here α is a streamwise wavenumber. For brevity, the full system of linearised equations describing the evolution of these perturbed flows is not given. The reader may refer to [5] for a form consistent with this work.

The amplification in kinetic energy over a given time interval $t = \tau$ can be written as a ratio of volume integrals over domain Ω of the inner products of $\boldsymbol{V}_p(t)$ at $t = \tau$ over the inital state at $t = 0$

$$G(\tau) = \frac{\int_\Omega \boldsymbol{V}_p(\tau)\cdot\boldsymbol{V}_p(\tau)\,\mathrm{d}V}{\int_\Omega \boldsymbol{V}_p(0)\cdot\boldsymbol{V}_p(0)\,\mathrm{d}V}. \quad (4)$$

A state-transition operator $\mathcal{A} = e^{Lt}$, where L is a linear operator, can be introduced to evolve an arbitrary initial perturbation $\boldsymbol{V}_p$ to time $t = \tau$ such that

$$\boldsymbol{V}_p(\tau) = \mathcal{A}(\tau)\boldsymbol{V}_p(0). \quad (5)$$

By further introducing an adjoint evolution operator $\mathcal{A}^*(\tau)$ of $\mathcal{A}$, that evolves an equivalent adjoint variable $\boldsymbol{V}_{p_\tau}^*$ backwards in time from $t = \tau$ to $t = 0$ (see [1] or [5] for further information), (4) can be rewritten as

$$G(\tau) = \frac{\int_\Omega \boldsymbol{V}_p(0)\cdot\mathcal{A}^*(\tau)\mathcal{A}(\tau)\boldsymbol{V}_p(0)\,\mathrm{d}V}{\int_\Omega \boldsymbol{V}_p(0)\cdot\boldsymbol{V}_p(0)\,\mathrm{d}V}. \quad (6)$$

In this form, the optimal growth $G(\tau)_{\max}$ is determined through the leading eigenvalue of the operator $\mathcal{A}^*\mathcal{A}$, with the corresponding optimal initial perturbation field given by the related eigenvector. Hence, the goal of the present work can be formally written as

$$G(\tau)_{\max} = \max_{\boldsymbol{V}_p(0)} \frac{\int_\Omega \boldsymbol{V}_p(0)\cdot\mathcal{A}^*(\tau)\mathcal{A}(\tau)\boldsymbol{V}_p(0)\,\mathrm{d}V}{\int_\Omega \boldsymbol{V}_p(0)\cdot\boldsymbol{V}_p(0)\,\mathrm{d}V}. \quad (7)$$

The global maximum amplification $G_{\max}$ occurs at the optimal time interval τ_{opt} having streamwise wavenumber α_{opt}.

Numerical Methodology

A high order spectral element method was employed to discretise the governing equations and implement the transient growth analysis methodology. The linearised component of this solver has been previously verified and implemented in works such as [10]. The reader may refer to [10] for further information regarding the numerical methodology. A grid resolution study was conducted to ensure adequate spatial and temporal sampling to accurately resolve the dynamics of the flow field. Streamwise wavenumbers were investigated between $0 \leq \alpha \leq 40$, with the local maxima resolved to an accuracy of at least 0.1. To ensure that the global maximum energy growths were captured, and a monotonic decay in amplifications were achieved at higher τ, the analysis was conducted over time intervals extending to $\tau = 100$. Eigenvalue convergence of better than 0.01% was ensured for all the values presented in this paper.

Results and Discussion

Global Maximum Amplifications for $10 \leq Ha \leq 1000$

The global maximum amplification occurring at τ_{opt} and α_{opt} as a function of Hartmann number for $10 \leq Ha \leq 1000$ are provided in figure 2. Here the results from [5] and [7] are also shown for comparison. Transient growth occurs for all Ha present in this study, however, the magnitude of these amplifications is progressively suppressed with increasing Hartmann number. This reduction in kinetic energy growth is most likely due to the increased magnetic damping found with higher Ha. For $10 \leq Ha \leq 100$ the global maximum amplification is described by the trend $G_{\max} \approx 11.45\times10^3 Ha^{-1.6}$. This is in close agreement with the $G_{\max} \approx 8.8\times10^3 Ha^{-1.5}$ relationship obtained by the optimal growth analysis in [5] over the limited range of $10 \leq Ha \leq 50$; serving as further validation for the numerical framework used in this study.

For $150 \leq Ha \leq 1000$ the optimal gain adopts a shallower decreasing trend with increasing Hartmann number. The results

demonstrate a remarkable consistency with the SM82 model data from [7]. For this higher Ha regime, the global maximum amplifications recover an approximate $-1/3$ power scaling with Hartmann number of $G_{\max} \approx 25 \times 10^3 Ha^{-0.37}$. However, for $Ha \leq 150$ there is a significant difference between those predicted by the SM82 analysis which will be investigated in more detail in the following section.

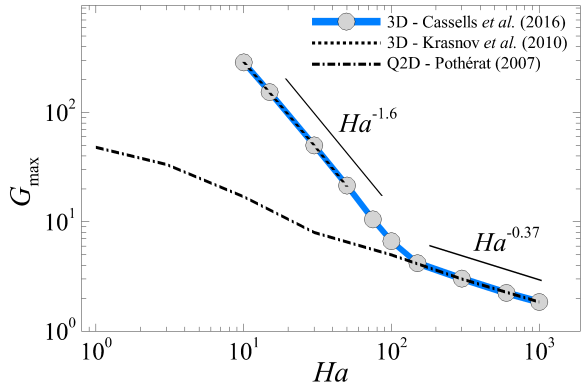

Figure 2: Global maximum amplifications as a function of Hartmann number. Here, pre-existing transient growth analysis data using a SM82 model [7] (dashed-dotted line) and quasi-static MHD analysis [5] (dash line) are plotted for comparison against current results (solid blue line).

Flow Visualisation and Perturbation Structures

The eigenvector fields for $Ha = 10, 100, 150$ and 600 are visualised via streamwise vorticity and two-dimensional slices of the streamwise component of velocity in figures 3 and 4, respectively. For larger Ha the perturbation structures become increasingly localised to the sidewall Shercliff layers (whose thickness scales with $Ha^{-1/2}$ [8]), and a significant decrease in the optimal streamwise wavenumber is also observed. The perturbation fields for low to moderate Ha form complex overlapping structures within the sidewall layers. Figure 4 (b) and (d) also demonstrate that for some cases the optimal perturbation fields are confined to only one boundary layer. As the core becomes largely uniform at higher Ha , interaction between boundary layer disturbances becomes diminished. Hence, whether the computed eigenmodes are isolated to one side-wall or occupying both side-walls, they are manifestations of the same optimal disturbance mode with identical energy amplification.

In the first regime between $0 \leq Ha \leq 100$, the eigenvector yielding the optimal disturbance field presents as roll-like structures aligned in the streamwise direction. As Ha is increased, the number of rolls in the spanwise direction also increase and become flattened within the thinning Shercliff layers. In the second regime between $150 \leq Ha \leq 1000$, a breakdown of the streamwise vortex structures occurs as highlighted in figures 3 (c) and (d). The flow becomes strongly invariant in the magnetic field direction, such that by $Ha = 600$ only remnants of streamwise vorticity remain and are confined to the corner regions of the duct. Figure 4 (c) and (d) further demonstrate this two-dimensionalisation, with relative invariance of w-velocity disturbance field near the side walls in the y-direction for $Ha \geq 150$.

The combination of this corner region localisation of streamwise vorticity and the relative invariance of w with y suggests that at higher Ha the perturbation kinetic energy

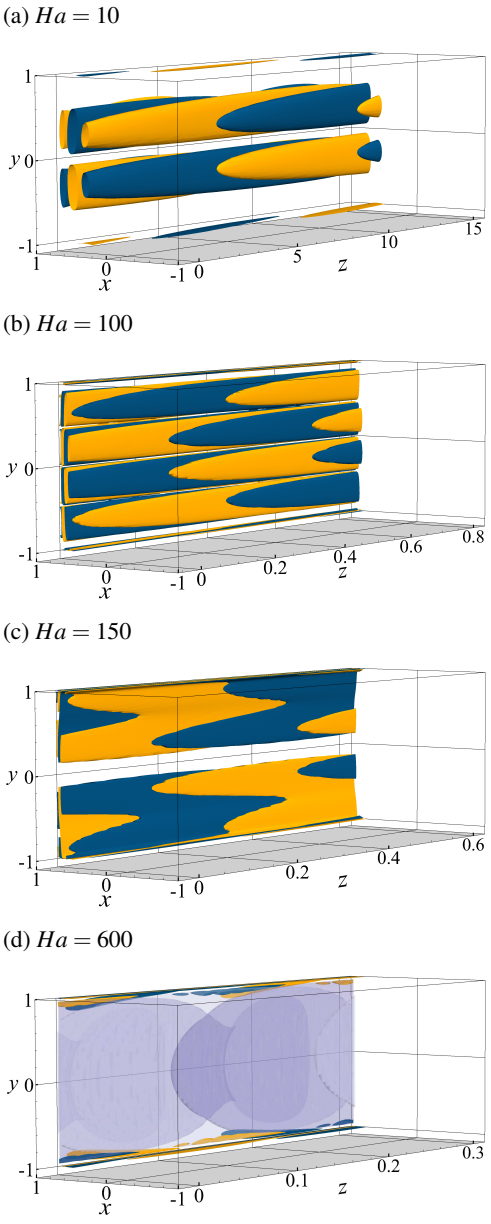

Figure 3: Eigenvector vorticity isosurfaces producing the maximum amplification $G_{\max}$ at τ_{opt} for $Ha = 10, 100, 150$ and 600 at $Re = 5000$. Blue and yellow contours represent positive and negative streamwise vorticity, respectively. Spanwise vorticity in the x-z plane are also visualised through purple isosurfaces in (d). Contour levels are adjusted to approximately 90% of the maximum magnitude of vorticity. The flow is from left to right in the positive z-direction, with the magnetic field orientated vertically in the positive y-direction. For clarity, the vorticity is only plotted for $0 \leq x \leq 1$.

is dominated by vertically aligned (Q2D) roll structures in the side-wall boundary layer (visualised by the purple x-z plane vorticity isosurfaces in figure 3 (d)). The mechanism producing maximum transient amplifications in low-Ha MHD flows and 3D Poiseuille flows result from the coupling of Orr-Sommerfeld and Squire modes; which in the context of the present configuration correspond to modes respectively invariant and variant in the vertical direction. The SM82 model, which can only combine the two-dimensional Orr–Sommerfeld modes for energy amplification, shows strong alignment of the 3D duct optimal growths predictions for $150 \leq Ha \leq 1000$.

Hence, in the limit of large Ha, the SM82 model is an excellent predictor of optimal linear growth when sufficient suppression of the Squire modes has occurred. Conversely, the coupling between these two mode types enhances the transient amplifications for $Ha \leq 150$, leading to the deviation between predicted growth rates as $Ha \to 0$. As Hartmann numbers in fusion reactor applications are typically quite large ($O(10^3)$), the ability of the SM82 model to accurately predict the dominant transient amplifications at these larger values allows for modelling to be conducted at significantly reduced computational costs, as the thin Hartmann layers (whose thickness scale with Ha^{-1} [8]) do not require resolving.

(a) $Ha = 10$

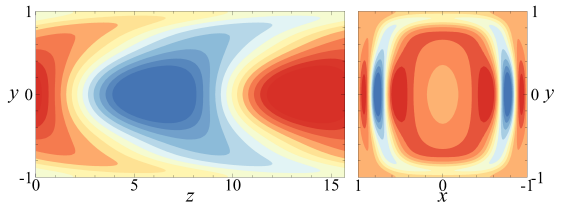

(b) $Ha = 100$

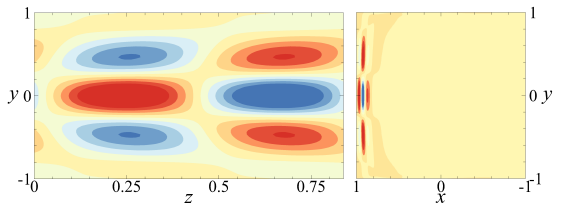

(c) $Ha = 150$

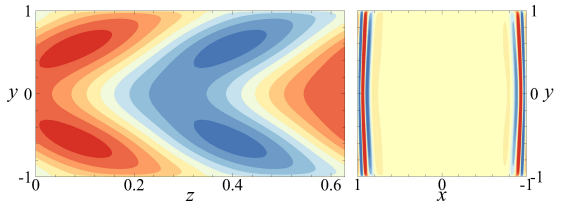

(d) $Ha = 600$

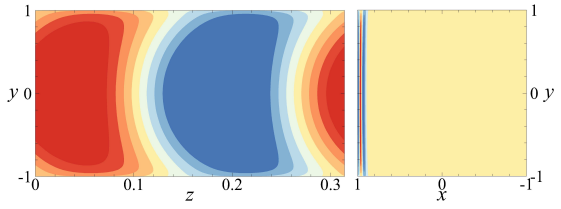

Figure 4: Contours of streamwise w-velocity plotted on representative x-planes (left) and z-planes (right) of the eigenvector fields producing $G_{\max}$ at τ_{opt} for $Ha = 10, 100, 150$ and 600 at $Re = 5000$. Red and blue contours represent positive and negative streamwise velocity, respectively. Contour levels are adjusted to approximately 90% of the maximum magnitude of w. The underlying base flow is in the positive z-direction, with the magnetic field orientated vertically in the positive y-direction.

Conclusions

The global maximum transient amplifications of an electrically conducting fluid under the influence of a transverse magnetic field were investigated. A range of Hartmann numbers for $10 \leq Ha \leq 1000$ were studied at a fixed $Re = 5000$. It was shown that two regimes exists for scaling of maximum transient growth amplification; when perturbation structures are dominated by 3D modes a scaling of $G_{\max} \propto Ha^{-1.6}$ for $10 \leq Ha \leq 100$ was found, and $G_{\max} \propto Ha^{-0.37}$ in the range of $150 \leq Ha \leq 1000$ for when optimal disturbances become predominantly Q2D. Through comparison with existing literature, the SM82 model for Q2D MHD flow is also shown to be a valid transient growth predictor in this regime.

Acknowledgements

O. G. W. C. was supported by an Engineering Research Living Allowance (ERLA) scholarship from the Faculty of Engineering, Monash University. This research was supported by Discovery Grant DP150102920 from the Australian Research Council, and was undertaken with the assistance of resources from the National Computational Infrastructure (NCI), which is supported by the Australian Government.

References

[1] Blackburn, H. M., Sherwin, S. J. and Barkley, D., Convective instability and transient growth in steady and pulsatile stenotic flows, *J. Fluid Mech.*, **607**, 2008, 267–277.

[2] Boeck, T., Krasnov, D., Thess, A. and Zikanov, O., Large-scale intermittency of liquid-metal channel flow in a magnetic field, *Phys. Rev. Lett.*, **101**, 2008, 244501.

[3] Cassells, O. G. W., Hussam, W. K. and Sheard, G. J., Heat transfer enhancement using rectangular vortex promoters in confined quasi-two-dimensional magnetohydrodynamic flows, *Int. J. Heat Mass Transfer*, **93**, 2016, 186–199.

[4] Hamid, A. H. A., Hussam, W. K. and Sheard, G. J., Combining an obstacle and electrically driven vortices to enhance heat transfer in a quasi-two-dimensional mhd duct flow, *J. Fluid Mech.*, **792**, 2016, 364–396.

[5] Krasnov, D., Zikanov, O., Rossi, M. and Boeck, T., Optimal linear growth in magnetohydrodynamic duct flow, *J. Fluid Mech.*, **653**, 2010, 273–299.

[6] Nraigh, L., Global modes in nonlinear non-normal evolutionary models: Exact solutions, perturbation theory, direct numerical simulation, and chaos, *Physica D*, **309**, 2015, 20–36.

[7] Pothérat, A., Quasi-two-dimensional perturbations in duct flows under transverse magnetic field, *Phys. Fluids*, **19**, 2007, 074104.

[8] Pothérat, A., Sommeria, J. and Moreau, R., An effective two-dimensional model for MHD flows with transverse magnetic field, *J. Fluid Mech.*, **424**, 2000, 75–100.

[9] Sommeria, J. and Moreau, R., Why, how, and when, MHD turbulence becomes two-dimensional, *J. Fluid Mech.*, **118**, 1982, 507–518.

[10] Tsai, T., Hussam, W. K., Fouras, A. and Sheard, G. J., The origin of instability in enclosed horizontally driven convection, *Int. J. Heat Mass Transfer*, **94**, 2016, 509–515.